Konrad-Zuse-Zentrum
für Informationstechnik Berlin

Takustraße 7
D-14195 Berlin-Dahlem
Germany

ANDREAS EISENBLÄTTER, HANS-FLORIAN GEERDES

Reconciling Theory and Practice: A Revised Pole Equation for W-CDMA Cell Powers

This work has been conducted within project B4 of the research center MATHEON "Mathematics for key technologies" in Berlin

ZIB-Report 07-11 (May 2007)

Reconciling Theory and Practice: A Revised Pole Equation for W-CDMA Cell Powers*

Hans-Florian Geerdes
Zuse Institute Berlin
Takustr. 7, 14195 Berlin
Germany
geerdes@zib.de

Andreas Eisenblätter
atesio GmbH
Sophie-Taeuber-Arp-Weg 27, 12205 Berlin
Germany
eisenblaetter@atesio.de

ABSTRACT

The performance evaluation of W-CDMA networks is intricate as cells are strongly coupled through interference. Pole equations have been developed as a simple tool to analyze cell capacity. Numerous scientific contributions have been made on their basis. In the established forms, the pole equations rely on strong assumptions such as homogeneous traffic, uniform users, and constant downlink orthogonality factor. These assumptions are not met in realistic scenarios. Hence, the pole equations are typically used during initial network dimensioning only. Actual network (fine-) planning requires a more faithful analysis of each individual cell's capacity. Complex analytical analysis or Monte-Carlo simulations are used for this purposes.

In this paper, we generalize the pole equations to include inhomogeneous data. We show how the equations can be parametrized in a cell-specific way provided the transmit powers are known. This allows to carry over prior results to realistic settings. This is illustrated with an example: Based on the pole equation, we investigate the accuracy of "average snapshot" approximations for downlink transmit powers used in state-of-the-art network optimization schemes. We confirm that the analytical insights apply to practice-relevant settings on the basis of results from detailed Monte-Carlo simulation on realistic datasets.

General Terms

Performance evaluation and modeling, Analytical Models, Formal methods for analysis of wireless systems

Keywords

W-CDMA, performance analysis, interference coupling, Monte-Carlo simulation, pole equation

*This work has been conducted within project B4 of the research center MATHEON "Mathematics for key technologies" in Berlin

1. INTRODUCTION

Third-generation cellular radio networks operating under the W-CDMA standard [7] frequently adapt to the current situation on the radio channel and user demand. In a power-control feedback loop, transmit powers are adjusted to the lowest possible level in order to overcome channel variations and avoid interference. This feature is essential, because all transmissions take place in one shared band—we are considering the single carrier case—and interference is a limiting factor. To determine the load of a system serving a given set of users is therefore an complex task. The performance of a radio cell depends on the position of its users as well as on the state of the cells in a large neighborhood.

For initial network dimensioning, a network planner needs to know how many users can be served simultaneously by the system. This question can be answered using pole equations for the down- and the uplink [12]. The main influences on network performance are roughly factored in and allow to derive a cell's pole capacity. Based on simplifying assumptions, the capacity of a single cell has been studied thoroughly with this approach and is now well understood. The underlying assumptions, however, are strong: users are uniformly distributed in hexagonal cells, interference coupling between cells is fixed, the downlink orthogonality loss factor does not vary, etc.

There have been attempts at formulating pole equations for a more general setting, or to derive alternative heuristic methods [6] for network evaluation. However, for detailed network planning—in realistic settings featuring inhomogeneous user distribution, a diverse traffic mix, non-uniform radio propagation conditions, and irregular cell layouts as illustrated in Fig. 1—these schemes provide a very coarse picture. To analyze the behavior of a network in detail, static system models have been devised [5]. These models allow an accurate account of network performance for a given set of users with arbitrary location and properties. The relation between cell powers can be described in linear interference coupling equation systems [9]. The solution of these systems describe the power equilibrium at which the system operates, assuming all demand to be served.

In the present contribution, we show how the intuitive form of the pole equation can be retained in an inhomogeneous setting. The formula is basically the same as before, only the parameter values are derived in a way that removes the simplifying assumptions. Using this technique, the analy-

sis of pole equations can now be applied during detailed, realistic network planning.

We demonstrate the usefulness of our concept by a practice-relevant example: In radio network planning and optimization [8, 7], the traditional, Monte-Carlo simulation technique is avoided for performance reasons. Various approximative techniques have been developed that trade evaluation accuracy for efficiency [13, 15]. A recent method for swiftly estimating cell performance within optimization schemes is to use an "average snapshot" [16, 11] or expected interference coupling [2]. The accuracy of this technique has been tested empirically [15], but not yet analyzed in theory. We use the revised pole equations for analysis and compare the results with Monte-Carlo simulation on realistic, inhomogeneous scenario data. It turns out that the analytical model predicts and explains the behavior in practice very well.

For brevity, we focus on the downlink direction in this work. The same technique, however, applies to the uplink.

2. CAPACITY OF W-CDMA NETWORKS

The downlink capacity required to serve users in a W-CDMA cell is measured in terms of the transmit power. Static systems models are commonly used to determine the average transmit power of a cell serving a given traffic *snapshot,* i. e., a set of users with specific demands and locations.

2.1 Static Models

We denote the average total downlink transmit power of a cell i serving a set M_i of users by $\bar{p}_i^{\downarrow}$ and the portion of this power spent on user m by $p_{im}^{\downarrow}$. In addition, the cell transmits common channels such as the pilot channel with a fixed power $p_i^{(\mathrm{C})}$. Denoting the activity factor of user m by $\alpha_m^{\downarrow}$, the average total power of cell i is calculated as

$$\bar{p}_i^{\downarrow} = \sum_{m \in M_i} \alpha_m^{\downarrow}\, p_{im}^{\downarrow} + p_i^{(\mathrm{C})} \tag{1}$$

For each user m the individual link power is adjusted such that a specified CIR-target $\mu_m^{\downarrow}$ is achieved.[1] Under the assumption of *perfect power control,* the ratio of link power over noise and interference is adjusted to precisely this value:

$$\mu_m^{\downarrow} = \frac{\gamma_{im}^{\downarrow}\, p_{im}^{\downarrow}}{\gamma_{im}^{\downarrow}\, \omega_m \left(\bar{p}_i^{\downarrow} - \alpha_m^{\downarrow}\, p_{im}^{\downarrow}\right) + \sum_{j \neq i} \gamma_{jm}^{\downarrow}\, \bar{p}_j^{\downarrow} + \eta_m^{\downarrow}} \tag{2}$$

where $\gamma_{im}^{\downarrow}$ is the end-to-end channel gain between cell i and user m, ω_m is the orthogonality loss factor applicable for the specific connection, and $\eta_m^{\downarrow}$ is the background noise (exterior to the system, including thermal noise). The parameters in (2) are user-specific and vary across a wide range. The transmit activity $\alpha^{\downarrow}$ and the CIR-target $\mu^{\downarrow}$ depend on the user's service; the path loss $\gamma_{im}^{\downarrow}$ and possibly the noise $\eta^{\downarrow}$ depend on the user's location; the orthogonality loss ω is also related to the user's environment.

[1]The CIR-target corresponds to the $\mathrm{E_b/N_0}$-target minus the processing gain:

$$\mu \;= \mathrm{E_b/N_0} \cdot \frac{\text{bit rate}}{\text{chip rate}}$$

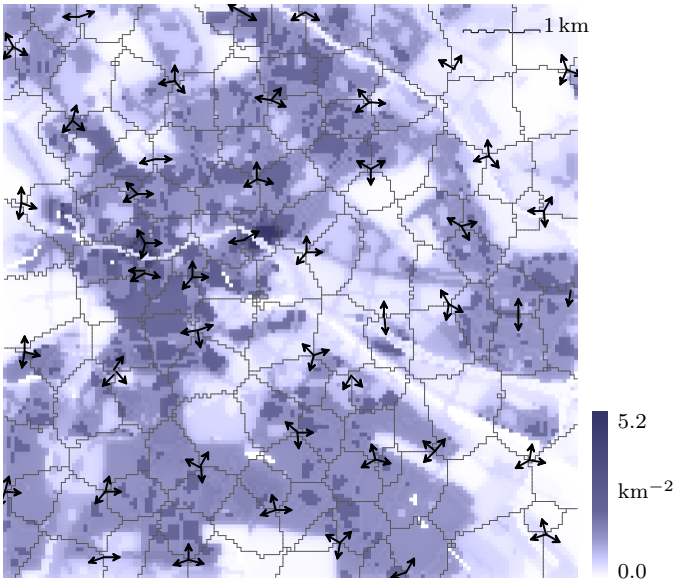

Figure 1: Network configuration, best server areas, and (normalized) downlink load distribution in the Berlin scenario: Realistic planning problems have irregular cell layout and inhomogeneous user load distribution

In some contributions ([12], for example), the own signal is fully accounted for as interference. The term $\bar{p}_i^{\downarrow}$ is then used in place of $(\bar{p}_i^{\downarrow} - \alpha_m^{\downarrow}\, p_{im}^{\downarrow})$ in the denominator of (2).

The set of all equations (1) for each cell and (2) for each user precisely describe the cell powers that prevail under perfect power control.

2.2 Network Load with Interference Coupling

The system of the equations (1) and (2) can be rewritten in a more condensed form by eliminating the individual link power variables $p_{im}^{\downarrow}$. Defining the load factor of user m as

$$\ell_m^{\downarrow} := \frac{\alpha_m^{\downarrow}\, \mu_m^{\downarrow}}{1 + \omega_m \alpha_m^{\downarrow}\, \mu_m^{\downarrow}}$$

we solve (2) for $\alpha_m^{\downarrow}\, p_{im}^{\downarrow}$ and obtain a variant of (1):

$$\bar{p}_i^{\downarrow} = \sum_{m \in M_i} \underbrace{\left(\ell_m^{\downarrow} \omega_m\, \bar{p}_i^{\downarrow} + \sum_{j \neq i} \ell_m^{\downarrow} \frac{\gamma_{jm}^{\downarrow}}{\gamma_{im}^{\downarrow}}\, \bar{p}_j^{\downarrow} + \ell_m^{\downarrow} \frac{\eta_m^{\downarrow}}{\gamma_{im}^{\downarrow}}\right)}_{=\alpha_m^{\downarrow}\, p_{im}^{\downarrow}} + p_i^{(\mathrm{C})} \tag{3}$$

We do not add the own signal as interference here. If the own signal is accounted for as interference, then $\alpha_m^{\downarrow}\mu_m^{\downarrow}$ needs to be substituted for $\ell_m^{\downarrow}$ instead of our definition (3). Modulo this modification, the same formula is derived in [7, 8, 12].

Let us introduce some notation to express this relation more compactly. We define the downlink coupling elements to be

$$c_{ii}^{\downarrow} := \sum_{m \in M_i} \omega_m \ell_m^{\downarrow} \qquad c_{ij}^{\downarrow} := \sum_{m \in M_i} \frac{\gamma_{mj}^{\downarrow}}{\gamma_{mi}^{\downarrow}} \ell_m^{\downarrow} \quad (j \neq i) \tag{4}$$

The coupling between pairs of cells is illustrated in Fig. 2.

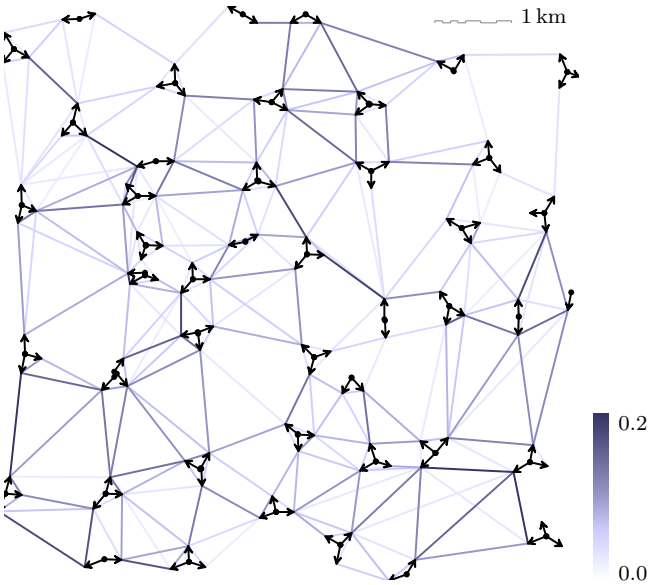

Figure 2: Interference-coupling between cells: Graphical representation of the off-diagonal entries in the interference-coupling matrix

In addition to cell coupling, we define the aggregated contributions of all mobiles to $\bar{p}_i^{\downarrow}$ that are independent of the cells' transmit powers as the *downlink noise load*

$$p_i^{(\eta)} := \sum_{m \in M_i} \frac{\eta_m^{\downarrow}}{\gamma_{im}^{\downarrow}} \ell_m^{\downarrow} \tag{5}$$

Then, equation (3) is equivalent to

$$\bar{p}_i^{\downarrow} = c_{ii}^{\downarrow} \bar{p}_i^{\downarrow} + \sum_{j \neq i} c_{ij}^{\downarrow} \bar{p}_j^{\downarrow} + p_i^{(\eta)} + p_i^{(\mathrm{C})} \tag{6}$$

In this form, the four different contributions to the cell's load are clearly laid out: capacity is needed to overcome intra-cell interference, inter-cell interference, and noise at the receiver.[2] In addition, there is the fixed power on the common channels.

The system of equation (6) for each cell is used for determining transmit powers in state-of-the-art network planning software tools. It can be shown that the solution is unique if a positive solution exists, see [14], for example.

2.3 Classical Pole Equation for Cell Capacity

An alternative version of interference coupling has been derived using the other-to-own-cell interference ratio. We follow the presentation for a downlink pole equation in [12]. Similar uplink versions exist [7]. The *other-to-own-cell interference* is a receiver-specific performance indicator classically defined as

$$f_m := \frac{\sum_{j \neq i} \gamma_{jm}^{\downarrow} \bar{p}_j^{\downarrow}}{\gamma_{im}^{\downarrow} \bar{p}_i^{\downarrow}} \tag{7}$$

An equivalent concept is the frequency reuse factor [1]. Using the other-to-own-cell interference ratio and rearranging terms in (3), we obtain an expression for the cell power equivalent to (6):

$$\bar{p}_i^{\downarrow} = \frac{p_i^{(\mathrm{C})} + \sum_m \eta_m^{\downarrow} \ell_m^{\downarrow} / \gamma_{im}^{\downarrow}}{1 - \underbrace{\sum_m \ell_m^{\downarrow} (\omega_m + f_m)}_{\text{downlink loading}}} \tag{8}$$

The classical pole equations are derived from (8) under idealizing assumptions. The first assumption is that all cells transmit with the same power. This is roughly true in a regular (e. g., hexagonal) scenario with uniform traffic. Secondly, a global orthogonality loss factor value $\bar{\omega}$ is used. Thirdly, there are N users, and all are assumed to have equal properties (corresponding to a common user load factor $\ell^{\downarrow}$). In this case, an average other-to-own-cell interference ratio can be defined as

$$\bar{f} := \frac{1}{N} \sum_m f_m = \frac{1}{N} \sum_m \sum_{j \neq i} \frac{\gamma_{im}^{\downarrow}}{\gamma_{jm}^{\downarrow}} \tag{9}$$

and an average path loss as

$$\frac{1}{\bar{\gamma}^{\downarrow}} := \frac{1}{N} \sum_m \frac{1}{\gamma_m^{\downarrow}} \tag{10}$$

Eq. (8) then reads as the classical pole equation:

$$\bar{p}^{\downarrow} = \frac{p^{(\mathrm{C})} + N \eta^{\downarrow} \ell^{\downarrow} / \bar{\gamma}^{\downarrow}}{1 - N \ell^{\downarrow} (\bar{\omega} + \bar{f})} \tag{11}$$

This equation has important applications. One example is the calculation of the approximate cell power needed to serve a given number of users [12]. Another one is that the system's pole capacity N_{pole} can be derived as the limit of the number of users served as transmit power tends to infinity:

$$N_{\mathrm{pole}} = 1 / \ell^{\downarrow} (\bar{\omega} + \bar{f}) \tag{12}$$

Numerous results have been obtained using variants of (11) and (12): the maximum number of users and maximum data rate in downlink have been calculated in [12]; the stochastic relation between user load and blocking and the trade-off between coverage and capacity in uplink has been investigated in [17]; the capacity of a cell for a given maximum blocking ratio has been determined in [18].

Some of the assumptions can be removed. For example, the inclusion of an arbitrary service mix is no problem. However, the results are not commonly used in detailed network planning because is is unclear how to find a suitable value for $\bar{f}$. The cell's average other-to-own-cell interference ratio varies considerably from cell to cell in inhomogeneous scenarios. This is illustrated in Fig. 3: the average other-to-own-cell interference ratio of cells is plotted over the normalized number of users in the cell. The computations have been made on the realistic network scenario[3] depicted in Fig. 1. Even after discarding outliers, the average other-to-own-cell interference ratio of most cells varies between 30 % and over 100 %.[4]

[2] In practice, the last contribution is negligible, as usually $p^{(\eta)} \ll p^{(\mathrm{C})}$.

[3] This is the Berlin scenario from the IST project MOMENTUM, available at `momentum.zib.de`.

[4] The depicted values are computed with the precise definition (14) below.

3. DECOMPOSING THE COUPLING EQUATION SYSTEM

From the interference coupling equation system we will now derive new parameter settings that remove unrealistic assumptions and that are valid for a slightly reformulated pole equation. If the cell powers are known (for example, by solving the coupling equation system), the specific values can be calculated for every cell.

3.1 Aggregated Other-to-own-cell Interference

The basis for our model is a definition of other-to-own-cell interference ratio that is slightly different from the classical one (7). We include the orthogonality loss factor that applies to the own-cell interference:

$$\tilde{\iota}_m^{\downarrow} := \frac{\sum_{j\neq i} \gamma_{jm}^{\downarrow} \bar{p}_j^{\downarrow}}{\omega_m \gamma_{im}^{\downarrow} \bar{p}_i^{\downarrow}} \tag{13}$$

This form lacks a direct physical interpretation, since the value ω captures an effect that is related to despreading the signal. In this way, however, connection-specific orthogonality values can be carried through the entire analysis in a concise fashion.

In contrast to the "naive" definition of an average other-to-own-cell interference ratio as the plain average over all users, we use a weighted average. The weight of a user is her contribution to the main diagonal element (4) of the coupling matrix. The aggregated other-to-own-cell interference ratio for cell i is then

$$\begin{aligned}\bar{\iota}_i^{\downarrow} &:= \frac{\sum_{m\in M_i} \omega_m \ell_m^{\downarrow} \tilde{\iota}_m^{\downarrow}}{\sum_{m\in M_i} \omega_m \ell_m^{\downarrow}} = \frac{\sum_{m\in M_i} \ell_m^{\downarrow} \sum_{j\neq i} \frac{\gamma_{jm}^{\downarrow}}{\gamma_{im}^{\downarrow}} \bar{p}_j^{\downarrow}}{\sum_{m\in M_i} \omega_m \ell_m^{\downarrow} \bar{p}_i^{\downarrow}} \\ &= \frac{\sum_{j\neq i} c_{ij}^{\downarrow} \bar{p}_j^{\downarrow}}{c_{ii}^{\downarrow} \bar{p}_i^{\downarrow}}\end{aligned} \tag{14}$$

Note that under the assumption of uniform transmit powers and identical users, the definition (14) is equivalent to (9) modulo orthogonality. (The average path loss (10) is accommodated in our definition of the noise power $p^{(\eta)}$.) Examples of average other-to-own-cell interference ratio in a realistic scenario are depicted in Fig. 3.

3.2 Pole Equation Revisited

Plugging the aggregated other-to-own-cell interference ratio (14) into the interference coupling equation (6), we obtain

$$\bar{p}_i^{\downarrow} = (1 + \bar{\iota}_i^{\downarrow})\, c_{ii}^{\downarrow} \bar{p}_i^{\downarrow} + p_i^{(\eta)} + p_i^{(\mathrm{c})} \tag{15}$$

By rearranging terms, we obtain the *revised pole equation:*

$$\bar{p}_i^{\downarrow} = \frac{p_i^{(\mathrm{c})} + p_i^{(\eta)}}{1 - (1 + \bar{\iota}_i^{\downarrow}) c_{ii}^{\downarrow}} \tag{16}$$

The expression $(1+\bar{\iota}_i^{\downarrow})c_{ii}^{\downarrow}$ is our notion of the *downlink loading* of cell i. We derive the following identity for $\bar{\iota}_i^{\downarrow}$:

$$\bar{\iota}_i^{\downarrow} = \frac{1 - (p_i^{(\eta)} + p_i^{(\mathrm{c})})/\bar{p}_i^{\downarrow}}{c_{ii}^{\downarrow}} - 1 \tag{17}$$

Eq. (17) provides a straightforward way of calculating $\bar{\iota}_i^{\downarrow}$ if transmit powers are known. If we use the maximum cell power $p_{\max}^{\downarrow}$ for $\bar{p}_i^{\downarrow}$, this defines a limit curve as indicated in Fig. 3. The curve basically expresses how a cell can serve a large number of users only if the level of interference is low.

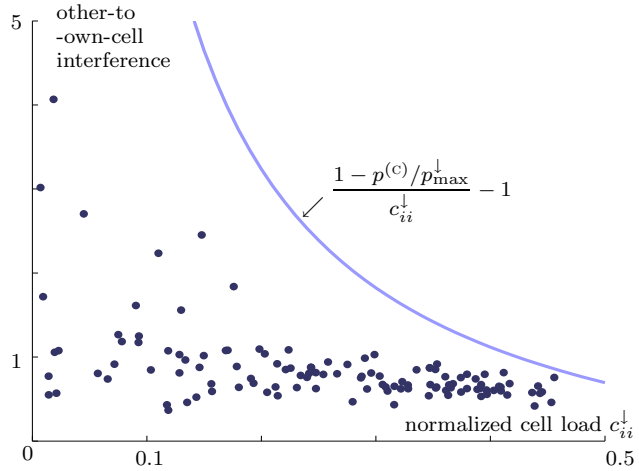

Figure 3: Other-to-own-cell interference values of cells in a real network vary greatly with local conditions; the solid line indicates the limiting value for serving a given load with restricted transmit power

Analogous to the classical analysis, the pole capacity of a cell is reached when the downlink loading approaches one. The transmit power then tends to infinity. In real networks, however, transmit powers are clipped at a limit $p_{\max}^{\downarrow}$ and excess demand is rejected by admission control. The actual transmit power in the cell is therefore

$$\bar{p}_i^{\downarrow} = \begin{cases} \frac{p_i^{(\mathrm{c})} + p_i^{(\eta)}}{1 - (1+\bar{\iota}_i^{\downarrow}) c_{ii}^{\downarrow}} & \text{if } (1+\bar{\iota}_i^{\downarrow}) c_{ii}^{\downarrow} < \frac{p_{\max}^{\downarrow} - p_i^{(\mathrm{c})} - p_i^{(\eta)}}{p_{\max}^{\downarrow}} \\ p_{\max}^{\downarrow} & \text{otherwise} \end{cases} \tag{18}$$

Here, we assume that admission control limits cell loading precisely to the maximum allowed value. The extension of the pole equation to reflect a more refined modeling of admission control is feasible using, for example, the concept of *perfect load control* as presented in [3].

4. APPLICATION: ANALYZING THE ACCURACY OF POWER ESTIMATES

This section presents an application of the refined downlink pole equation. We analyze the accuracy of an "average snapshot" approximation for estimating cell transmit powers. This technique, also called *expected interference-coupling approximation,* is used to obtain estimates for average transmit powers if Monte-Carlo simulation is too time consuming. This is, for example, the case if search methods such as simulated annealing are used for network optimization and many candidate configurations have to be tested in a short time [16, 2].

4.1 Expected Coupling of Transmit Powers

In the expected interference-coupling approach, a single system of equations of type (6) is solved to obtain the average coupling values. For a reference service with user load factor $\ell_r^{\downarrow}$ and spatial user density $T(\cdot)$, the mean coupling values

are calculated as integrals over the area A_i of cell i:

$$\bar{c}_{ii}^{\downarrow} := \mathbb{E}(c_{ii}^{\downarrow}) = \int_{A_i} \omega_p \ell_r^{\downarrow} T(p)\,\mathrm{d}p \tag{19a}$$

$$\bar{c}_{ij}^{\downarrow} := \mathbb{E}(c_{ij}^{\downarrow}) = \int_{A_i} \frac{\gamma_{pj}^{\downarrow}}{\gamma_{pi}^{\downarrow}} \ell_r^{\downarrow} T(p)\,\mathrm{d}p \quad (i \neq j) \tag{19b}$$

$$\bar{p}_i^{(\eta)} := \mathbb{E}(p_i^{(\eta)}) = \int_{A_i} \frac{\eta_p^{\downarrow}}{\gamma_{ip}^{\downarrow}} \ell_r^{\downarrow} T(p)\,\mathrm{d}p \tag{19c}$$

The computation assumes that a user is always served by the cell providing the strongest signal (best server). Variations of the radio channel, i. e., stochastic attenuation values γ, are not considered. If fading is taken into account, the cell areas vary according to the current radio conditions and the expected coupling elements can only be computed by numerical integration [13, 15]. The mean coupling value for a service mix is the sum over the individual components for the services.

In the remainder of this paper, we analyze the error in estimating the cell transmit powers $\bar{p}^{\downarrow}$ using expected interference-coupling approach in comparison to simulation results. While similar investigations have been conducted before, our analysis based on the pole equation sheds a new light on the factors governing the estimation error.

4.2 Simplified Setting

We consider one cell with a fixed average other-to-own-cell interference ratio of $\hat{\imath}^{\downarrow}$. The following assumptions are made: noise is neglected (i. e., $p^{(\eta)} = 0$); all m users in the snapshot wish to access a reference service r with a user load factor of $\ell_r^{\downarrow}$ (i. e., all users have exactly the same impact on the system and a snapshot is completely described by its number of users); load control admits the maximum number of users $m^* \leq m$ for which the system load is still within the desired bounds.

The coupling element is calculated as

$$c^{\downarrow}(m) = m^* \ell_r^{\downarrow}$$

The pole equation for m users then reads

$$\bar{p}^{\downarrow}(m) = \frac{p^{(\mathrm{C})}}{1 - (1+\hat{\imath}^{\downarrow})\ell_r^{\downarrow} m^*} \tag{20}$$

The maximum number of admissible users is calculated by setting $\bar{p}^{\downarrow} = p_{\max}^{\downarrow}$ in (20):

$$m^{(\max)} := \frac{p_{\max}^{\downarrow} - p^{(\mathrm{C})}}{p_{\max}^{\downarrow}(1+\hat{\imath}^{\downarrow})\ell_r^{\downarrow}}$$

Hence, the system will admit exactly

$$m^* = \min(\lfloor m^{(\max)} \rfloor, m)$$

users. The load factor (before admission control) is

$$(1+\bar{\imath}^{\downarrow})\ell_r^{\downarrow} m$$

We assume the number of users to be Poisson-distributed. The probability that exactly m users are present is

$$\mathrm{P}(m) = \phi^m e^{-\phi}/m!$$

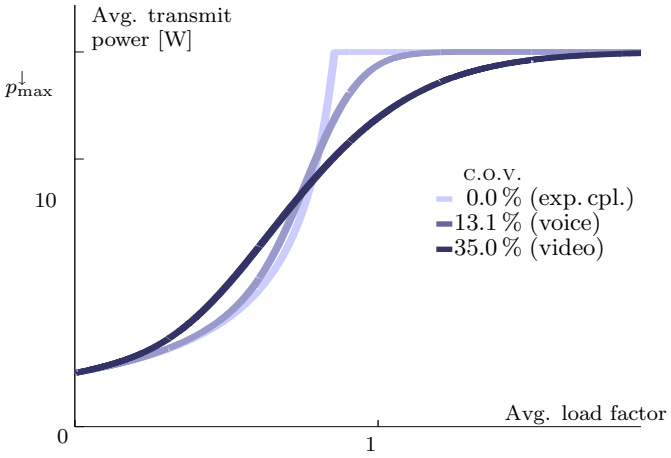

Figure 4: Theoretical analysis of average transmit power vs. load factor for different traffic mixes

where $\phi \geq 0$ is the average number of users in the cell. As the number of users is the only random influence, the expected load factor is

$$\mathbb{E}((1+\bar{\imath}^{\downarrow})\ell_r^{\downarrow} m) = (1+\bar{\imath}^{\downarrow})\ell_r^{\downarrow}\phi \tag{21}$$

and its variance is

$$\mathrm{Var}((1+\bar{\imath}^{\downarrow})\ell_r^{\downarrow} m) = (1+\bar{\imath}^{\downarrow})^2 \left(\ell_r^{\downarrow}\right)^2 \phi \tag{22}$$

The true values for the expected powers thus are

$$\begin{aligned}\mathbb{E}(\bar{p}^{\downarrow}) = &\textstyle\sum_{m \leq m^{(\max)}} \mathrm{P}(m)\bar{p}^{\downarrow}(m) \\ &+ \textstyle\sum_{m > m^{(\max)}} \mathrm{P}(m)\bar{p}^{\downarrow}(\lfloor m^{(\max)} \rfloor)\end{aligned} \tag{23}$$

The latter sum is an infinite series that converges necessarily. The mean of the coupling element, on the other hand, is

$$\mathbb{E}(c^{\downarrow}) = \phi \ell_r^{\downarrow}$$

The expected-coupling estimates in the decoupled case are therefore calculated according to (18) as

$$\bar{p}^{\downarrow} = \begin{cases} \frac{p^{(\mathrm{C})}}{1-(1+\hat{\imath}^{\downarrow})\ell_r^{\downarrow}\phi} & \text{if } \phi \leq m^{(\max)} \\ p_{\max}^{\downarrow} & \text{otherwise} \end{cases} \tag{24}$$

Based on (24), we study the impact of user load "granularity" on the average cell transmit in the next section.

4.3 Analysis

The values in (23) and the expected-coupling estimates (24) for $\bar{p}^{\downarrow}$ are exemplarily calculated with the parameter settings

$$p^{(\mathrm{C})} = 2\,\mathrm{W} \quad p_{\max}^{\downarrow} = 14\,\mathrm{W} \quad \hat{\imath}^{\downarrow} = 1.08 \quad \ell_r^{\downarrow} = 0.059, 0.008$$

The first choice for $\ell_r^{\downarrow} = 0.008$ corresponds to a speech service with 50 % activity; the second value $\ell_r^{\downarrow} = 0.059$ is realistic for a video call service with 100 % activity. The parameters have been chosen such that $m^{(\max)}$ is integral.

The abscissa in Fig. 4 shows the mean load factor as stated in (21). The three curves differ only in the variance (22) of the load factor. Due to the fixed other-to-own-cell interference ratio, the variance is determined by the service. At the

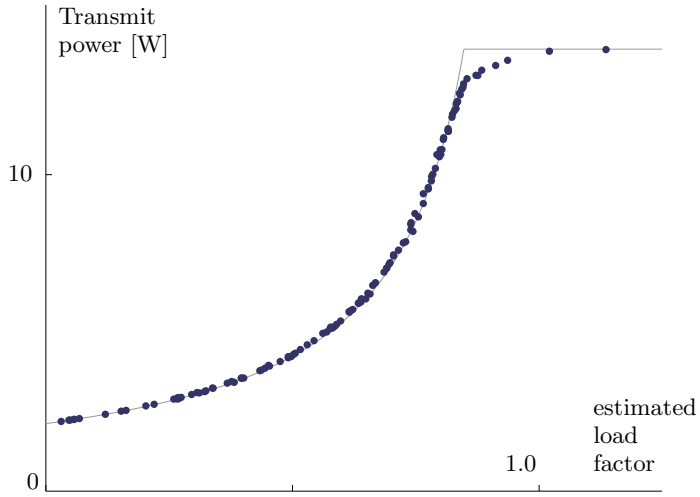

(a) Speech service only: the simulation results correspond to the middle curve from Fig. 4, the main inaccuracy of the estimates is the overestimation for high load factors

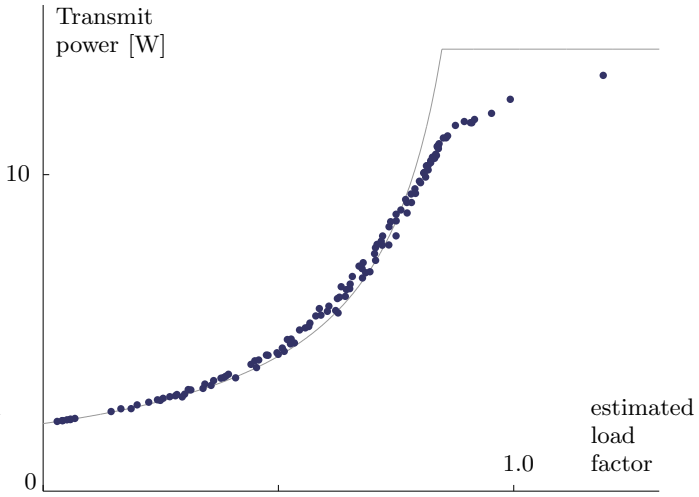

(b) Differentiated service mix: accuracy behaves as predicted in theoretical analysis – higher underestimation for low load factors and higher overestimation for high load factors

Figure 5: Monte-Carlo simulation results (dots) for mean downlink transmit powers vs. estimates (solid line), Berlin scenario

same expected load, the more demanding video service leads to a higher variance. The curves in Fig. 4 are thus labeled by their *coefficient of variation* (C.O.V.), which is calculated as the ratio of the standard deviation over the mean.

Fig. 4 reveals that expected-coupling approximations underestimate the power for a low average load factor. For high load factors, the average power is overestimated. This is easily explained: When the average load factor is low, blocking virtually plays no role. As the power is a strongly convex function of the load factor, the situations with more than average many users influence the mean more heavily than those with fewer than average. In the region with "expected overload", on the other hand, expected-coupling approximation ignores the fact that those snapshots for which the maximum power is *not* reached have a positive probability. If the load factor has zero variance, the expected-coupling estimate is exact. The higher the variance of the load factor, the more pronounced is the deviation of actual values from our estimate. This holds for the underestimation at low load as well as for overestimation at high load.

5. COMPUTATIONAL VALIDATION

We conducted experiments on realistic data to validate the insights from theoretical analysis. We do not provide a fully-fledged quantitative statistical analysis of our results, as this can be carried out without using our theoretical insights. Similar computational tests (but not containing the above analysis) are in fact presented in [15] for a classical hexagonal setting and led to comparable results. Instead, we stress how the analysis of the pole equation explains effects observed under realistic conditions.

5.1 Scenarios

We carried out Monte-Carlo simulations on two realistic public planning data provided by the MOMENTUM project [4, 10]. The network configuration, traffic intensity, and service mix were varied. The normalized downlink traffic intensity (aggregated user load) is based on population data, which is spatially inhomogeneous. The distribution is indicated in Fig. 1 for the Berlin scenario; the peak value of 5.2 corresponds to about 650 speech users per square kilometer. The traffic distribution for Lisbon is shown in Fig. 6.

Two service mixes are considered: an all-speech one as well as a differentiated mix featuring 56 % speech load, 7 % video load, and a variety of downlink-biased data services (such as WWW, download, email) for the residual users. Both traffic mixes are adjusted to create a comparable total load and differ mainly in the variance of user load. The radio propagation predictions are based on a Okumura-Hata model including diffraction based on terrain height data and clutter type. The data has a resolution of 50×50 m (Berlin) and 20×20 m (Lisbon).

We present results for two specific network configurations depicted in Figs. 1 and 6. The results for various network configurations are comparable at a qualitative level. As can be seen in the figures, the irregular placement of base stations and propagation data cause an irregular cell layout.

5.2 Simulation vs. Expected Coupling

We compare the results from Monte-Carlo simulation with expected-coupling estimates. The convergence criterion for simulation was based on confidence intervals for individual cell powers. The intervals have been computed on the assumption of a lognormal power distribution of the cell powers [18]. The simulation has been run until the 99 % confidence interval was less than ± 1 % of the mean. Results for the two service mixes in Berlin are shown in Fig. 5 and for the differentiated service mix in Lisbon in Fig. 7. Each dot represents the result for one cell, its ordinate is the average power as determined by simulation. The abscissae is

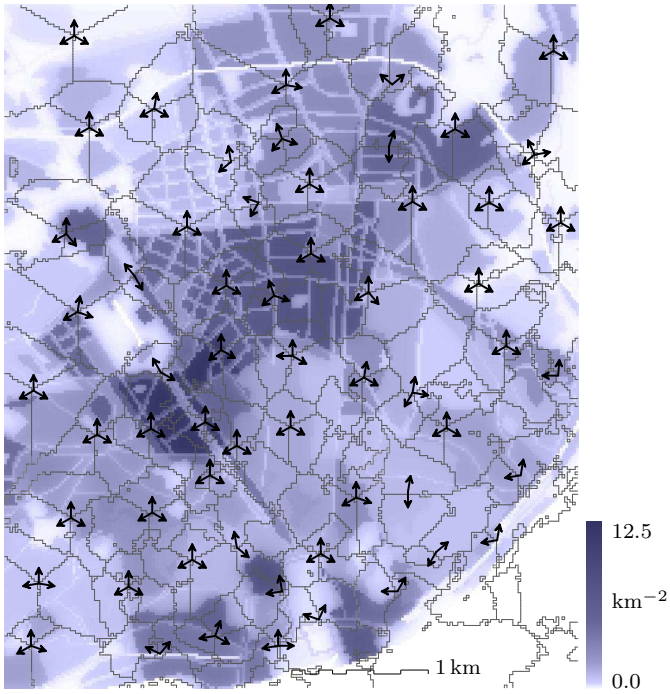

Figure 6: Irregular cell layout and inhomogeneous downlink load distribution (normalized), Lisbon scenario

the approximation for expected downlink loading $(1+\bar{\iota}_i^{\downarrow})c_{ii}^{\downarrow}$ as estimated by expected-coupling analysis. The expected-coupling estimate for downlink power is a function of this value, which is specified in equation (18). The estimated power is indicated in the plots by the light solid line.

Fig. 5(a) shows the accuracy of expected-coupling estimates in the Berlin scenario for the case of only speech users. A cell can typically handle 50 speech users simultaneously. Since user load is of a fine granularity, the variance of a cell's load factor is rather low and the dots lie close to the line indicating the estimates. As predicted by the analysis, the largest estimation errors occur in regions of the higher load: the average cell power is estimated as the maximum value $p_{\max}^{\downarrow}$, but the value observed in simulation is slightly lower.

The precision of expected-coupling estimates for the complete service mix is shown in Fig. 5(b). The dots deviate more heavily from the curve. This is because there are fewer users, but they are more demanding, which increases the granularity of users. The variance of the load factor is hence larger, and the points deviate more from the curve. This happens as predicted by the analysis: for lower load values, there is more underestimation, whereas in highly loaded cells, the overestimation is larger. In general, the bias of estimation error is towards overestimation.

The bottom line is the following: the difference in accuracy of estimates for different service mixes observed between Figs. 5(a) and (b) is explained by the analysis presented in this paper. Fig. 5(a) corresponds to the "speech" curve in Fig. 4, and Fig. 5(b) to the "video" curve for higher variance. This was observed in all our experiments; Fig. 7

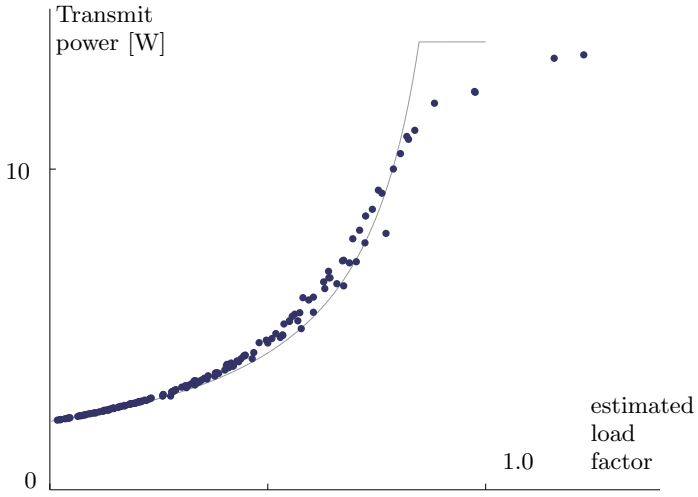

Figure 7: Monte-Carlo simulation results (dots) for mean downlink transmit powers vs. estimates (solid line), Lisbon scenario. Also in this setting, experiments confirm the theoretical analysis

contains comparable results in the Lisbon scenario (which is significantly different from the Berlin scenario) for the differentiated service mix.

Our results can also be used for calculating more accurate estimates for the average transmit power, if this is of interest: Based on the service mix and user distribution, the variance of the load factor can be estimated. A corresponding curve from Fig. 4 can be used as a finer approximation than the solid lines in Figs. 5 and 7, which assume vanishing variance. This is, however, out of the scope of the present work.

5.3 Impact of Shadow Fading

The experiments conducted so far have not included variations of the radio channel, i. e., fading effects. We now study the impact of log-normal fading using a model with angular correlation [19] and a standard deviation of 8 dB.

The main consequence of shadowing is that cell areas vary (if we assume a best-server connection). This implies that the values calculated in (19) are no longer the mean of the coupling elements. We address two questions: First, how well do expected-coupling estimates with medians of attenuation approximate average transmit powers? Second, how do precise expected-coupling estimates perform?

No closed formula is known for calculating the mean of the coupling matrix in the presence of shadowing; the existing methods [13, 15] require numerical integration of multi-dimensional functions. For our results, we determine the mean by Monte-Carlo simulation.

Examples for the Berlin network are shown in Fig. 8. Fig. 8(a) depicts results for the expected-coupling method with medians of attenuation. The abscissae (load estimates) of the data points are identical to those in Fig. 5(b). Because the simulation now includes shadowing, the ordinates (observed power) are different. The points are more scattered. The

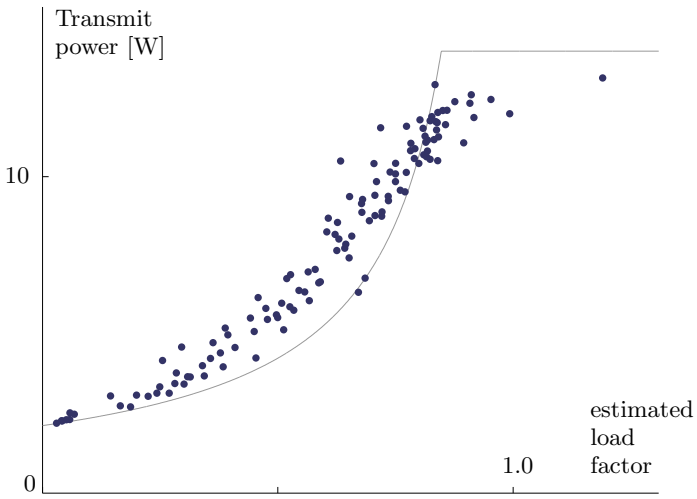

(a) If fading is considered, the simulation results are scattered compared to the expected-coupling estimates using medians of attenuation. The general trend is captured, but individual cells deviate strongly

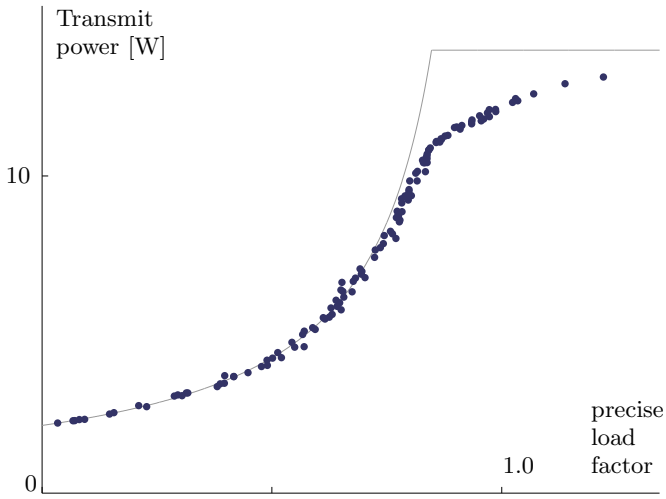

(b) The same results as in (a) rearranged according to the precise average downlink loading value from simulation: the curve agrees with the theoretical analysis

Figure 8: Simulation results including shadowing (dots) and estimates (solid line) for downlink transmit power, differentiated service mix

general tendency is similar: cells with low (estimated) loading tend to expose a higher average transmit power than estimated, while highly-loaded cells have less. In general, the loading is higher with shadowing.

Fig. 8(b) depicts the results for a "exact" determination of mean coupling elements. As the simulation is identical, the ordinates (power values) of the cells' data points are identical to those in Fig. 8(a). The estimates of mean loading, the abscissae, however, are different. This is because the precise values are used. It can be observed that the estimates for transmit powers are far more accurate if the computationally expensive estimates are afforded. The picture is similar to Fig. 5(b), the main difference being that underestimation virtually does not occur anymore. This is because the overall loading is higher under shadowing, so overestimation prevails and this also influences the almost empty cells through interference coupling.

6. CONCLUSION

The classical pole equations are a popular tool for cell capacity analysis as they describe the behavior of a W-CDMA cell in an accessible way. In particular, the effects of stochastic variations of the user load have been extensively studied. We have formulated an alternative version of the classical downlink pole equation. The alternative version differs only slightly from the classical definition. This allows to carry over all analytical insights obtained in the classical model.

The main achievement of the present contribution is an alternative definition of the parameters in the pole equations, notably of a cell's average other-to-own-cell interference ratio, which accommodates all information of a detailed planning scenario. With these generalized definitions, the classical pole equation can be parameterized to the precise working point of a specific cell in a realistic scenario. As a consequence, all results obtained by analysis of the pole equation—most prominently, stochastic results—can be directly used in practical, detailed network planning.

As one example for this technique, we have provided an analysis of the accuracy of a method for quickly estimating cell transmit powers. This method is used in state-of-the-art network optimization. The so-called expected-coupling estimates determine the transmit power for a hypothetical "average snapshot" and can be calculated very efficiently. Costly Monte-Carlo simulation is avoided. Based on the pole equations, we have pointed out how the service mix influences the variation of the downlink loading and thereby the accuracy of the estimates. The results of this analysis have been shown to apply with surprising accuracy in a realistic planning scenario featuring irregular traffic distribution and cell layout. Our results furthermore highlight how higher-order moments may be efficiently used for more precise estimates.

7. REFERENCES

[1] S. Dehghan, D. Lister, R. Owen, and P. Jones. W-CDMA capacity and planning issues. *Electron. & Comm. Eng. J.*, 12(3):101–118, June 2000.

[2] A. Eisenblätter, H.-F. Geerdes, T. Koch, A. Martin, and R. Wessäly. UMTS radio network evaluation and optimization beyond snapshots. *Math. Methods Oper. Res.*, 63:1–29, Mar. 2006.

[3] A. Eisenblätter, H.-F. Geerdes, and N. Rochau. Analytical approximate load control in WCDMA radio networks. In *Proc. VTC-2005 Fall*, Dallas, TX, Sept. 2005. IEEE.

[4] A. Eisenblätter, H.-F. Geerdes, and U. Türke. Public UMTS radio network evaluation and planning scenarios. *Internat. J. Mobile Network Des. and Innovation*, 1(1):40–53, 2005.

[5] A. Eisenblätter, T. Koch, A. Martin, T. Achterberg, A. Fügenschuh, A. Koster, O. Wegel, and R. Wessäly. Modelling feasible network configurations for UMTS. In G. Anandalingam and S. Raghavan, editors, *Telecommunications Network Design and Management*, pages 1–22. Kluwer, 2002.

[6] B. Heideck, A. Draegert, and T. Kürner. Heuristics for the reduction of complexity in UMTS radio network quality assessment. In *Proc PIMRC 2002*, volume 1, pages 320–324, 2002.

[7] H. Holma and A. Toskala, editors. W-CDMA *for* UMTS. Jon Wiley & Sons, revised edition, 2001.

[8] J. Laiho, A. Wacker, and T. Novosad, editors. *Radio Network Planning and Optimisation for* UMTS. John Wiley & Sons, 2002.

[9] L. Mendo and J. M. Hernando. On dimension reduction for the power control problem. *IEEE Trans. Comm.*, 49(2):243–248, Feb. 2001.

[10] MOMENTUM project. Public UMTS radio network planning scenarios. Available online at `http://momentum.zib.de/data`, 2003.

[11] C. Murphy, M. Dillon, and A. Diwan. Performance gains using remote control antennas in CDMA and 1xEV-DO networks. In *Proc IEEE VTC Fall 2005*, Dallas, TX, USA, Sept. 2005.

[12] K. Sipilä, K. Honkasalo, J. Laiho-Steffens, and A. Wacker. Estimation of capacity and required transmission power of W-CDMA downlink based on a downlink pole equation. In *Proc. VTC Spring 2000*, Tokyo, Japan, 2000.

[13] D. Staehle. *Analytical Methods for* UMTS *Radio Network Planning*. PhD thesis, Bayerische Julius-Maximilian-Universität Würzburg, Würzburg, Germany, 2004.

[14] S. Stańczak, M. Wiczanowski, and H. Boche. *Resource Allocation in Wireless Networks*. LNCS. Springer, 2006.

[15] U. Türke. *Efficient Methods for* W-CDMA *Radio Network Planning and Optimization*. PhD thesis, Universität Bremen, 2006.

[16] U. Türke and M. Koonert. Advanced site configuration techniques for automatic UMTS radio network design. In *Proc IEEE VTC Spring 2005*, Stockholm, Sweden, 2005.

[17] V. V. Veeravalli and A. Sendonaris. The coverage-capacity tradeoff in cellular CDMA systems. *IEEE Trans. Veh. Technol.*, 48(5):1443–1450, 1999.

[18] A. M. Viterbi and A. J. Viterbi. Erlang capacity of a power controlled CDMA system. *IEEE J. Sel. Area Comm.*, 11(6):892–900, 1993.

[19] T. Winter, U. Türke, E. Lamers, R. Perera, A. Serrador, and L. Correia. Advanced simulation approach for integrated static and short-term dynamic UMTS performance evaluation. Technical Report D27, MOMENTUM IST-2000-28088, 2003.